

## Growth, structural, and physical properties of superconducting $\text{Nd}_{2-x}\text{Ce}_x\text{CuO}_4$ crystals

J.-M. Tarascon, E. Wang, L. H. Greene, B. G. Bagley, G. W. Hull,  
S. M. D'Egidio, and P. F. Miceli  
*Bellcore, 331 Newman Springs Road, Red Bank, New Jersey 07701*

Z. Z. Wang, T. W. Jing, J. Clayhold, D. Brawner, and N. P. Ong  
*Department of Physics, Princeton University, Princeton, New Jersey 08544*  
(Received 24 April 1989)

Single crystals of the  $n$ -type Nd-Ce-Cu-O superconducting materials have been grown via a flux technique, and their structural and physical properties characterized. Optimum crystal growth conditions were arrived at from a survey of various compositions and temperatures. We determine that the charge composition (50 mol %  $\text{Nd}_2\text{O}_3$ - $\text{CeO}_2$ , 50 mol %  $\text{CuO}$ ) held at a temperature of  $1300^\circ\text{C}$  and followed by a slow cooling to  $1000^\circ\text{C}$  produces plateletlike crystals of the  $n$ -type phase  $\text{Nd}_{2-x}\text{Ce}_x\text{CuO}_4$ , which, after being annealed at  $900^\circ\text{C}$  in nitrogen, become superconducting. The limit of the Ce solubility is  $x=0.18$ , and only crystals having a Ce content between 0.14 and 0.17 were found to be superconductors, with the maximum  $T_c$  occurring at  $x=0.14$ . The oxygen uptake and loss in the Nd material is similar to that measured on  $\text{La}_2\text{CuO}_4$  but occurs at higher temperatures ( $750^\circ\text{C}$  instead of  $500^\circ\text{C}$ ). The large Meissner fraction indicates bulk superconductivity. However, due to a complex microstructure or compositional (e.g., oxygen) inhomogeneities in the crystal, zero resistance is difficult to achieve. The resistivity temperature dependence above  $T_c$  is metalliclike, and linear above 150 K, in contrast to bulk ceramics. Finally, no evidence for magnetic ordering over the temperature range 4–350 K was observed for the superconducting Ce-doped  $\text{Nd}_2\text{CuO}_4$  phase, whereas signs of magnetic ordering were found at 340 K for the undoped material.

### INTRODUCTION

Following the initial discovery by Bednorz and Muller<sup>1</sup> of superconductivity at 34 K in the La-Ba-Cu-O system there have been several new superconducting cuprates discovered having transition temperatures ( $T_c$ ) from 10 K to as high as 125 K.<sup>2–5</sup> A structural feature common to all of these compounds, which belong to the perovskite family, is that they contain  $\text{CuO}_2$  planes. The Cu valence (formal) in these materials, which can be easily changed by either the removal or uptake of oxygen or by certain cationic substitutions, is a crucial parameter for the appearance of superconductivity. Until recently only those chemical substitutions that lead to a Cu formal valence greater than 2 have produced superconducting compounds (e.g., insulating  $\text{La}_2\text{CuO}_4$  doped with Sr leads to a 40 K superconducting  $\text{La}_{2-x}\text{Sr}_x\text{CuO}_4$ , Refs. 6–8). The formation of Cu with a valence greater than 2 (i.e., oxidation of Cu) implies the introduction of a hole charge state. These holes, or missing electrons, are the charge carriers in all these cuprate superconductors and they are called, for this reason,  $p$  type.

Recently Tokura *et al.*<sup>9</sup> discovered a new class of materials  $\text{Nd}_{2-x}\text{Ce}_x\text{CuO}_4$  which are  $n$ -type superconductors at 23 K. They did this by chemically reducing the Cu (i.e., doping the system with electrons) in two steps: (1) the replacement of trivalent (Nd) by tetravalent ions (Ce), and (2) the removal of oxygen. This new superconducting phase still contains  $\text{CuO}_2$  planes, but the carriers are electrons ( $n$  type) and not holes ( $p$  type). The  $n$ -type character has been determined by Hall and Seebeck mea-

surements,<sup>10</sup> and x-ray absorption measurements<sup>11</sup> on polycrystalline samples indicate the presence of  $\text{Cu}^+$  scaling with Ce. Additional evidence supporting  $n$ -type conductivity in these new electron-doped superconductors is that the replacement of oxygen by fluorine (i.e., again a reduction of the Cu) also induces superconductivity.<sup>12</sup> By replacing the Nd in the parent compound  $\text{Nd}_{2-x}\text{Ce}_x\text{CuO}_4$  by other rare earths (Pr, Sm, Eu), and the Ce by Th, additional new  $n$ -type superconducting phases have been synthesized.<sup>13,14</sup>

One major experimental aspect concerning these new  $n$ -type superconductors is that the Meissner fractions thus far observed are small. This suggests that these initial ceramic samples are either inhomogeneous or contain secondary phases. A similar conclusion is arrived at from the shape of the resistance versus temperature plot which, for the best superconducting ceramic so far reported, is semiconductinglike above  $T_c$ . Thus higher-quality homogeneous ceramics or single crystals of these compounds are required to ensure that bulk  $n$ -type superconductivity exists in this system and to provide more reliable experimental data. We report here on the growth of  $\text{Nd}_{2-x}\text{Ce}_x\text{CuO}_4$  crystals and their structural, transport, and magnetic properties in comparison to those of ceramic samples. These  $n$ -type crystals, which are superconducting at 23 K and show a metalliclike conductivity above  $T_c$ , are grown using a flux method.

### EXPERIMENTAL

$\text{Nd}_{2-x}\text{Ce}_x\text{CuO}_4$  polycrystalline ceramics with  $x$  ranging from 0 to 0.5 in steps of 0.05 were prepared as fol-

lows: Stoichiometric mixtures of  $\text{Nd}_2\text{O}_3$ ,  $\text{CuO}$ , and  $\text{CeO}_2$  (all 5N) were heated to  $900^\circ\text{C}$  in air for 16 h, ground, and then fired at  $1100^\circ\text{C}$  for 24 h. After such a treatment the samples are single phase up to a cerium content,  $x$ , of 0.2. Within this concentration range the variation of the lattice parameters (shown in Fig. 1) is similar to that reported by Takagi *et al.*<sup>10</sup> The unit-cell volume decreases with increasing Ce content at low  $x$  (because of the smaller ionic radius of  $\text{Ce}^{4+}$  compared to  $\text{Nd}^{3+}$ ) and levels off between  $x = 0.2$  and 0.25, most likely because the solubility limit of Ce was exceeded. This agrees with our observation of several extra Bragg peaks corresponding to  $\text{CeO}_2$  in the powder-diffraction patterns of samples with  $x > 0.2$ . We observe that the range of solubility of Ce in  $\text{Nd}_2\text{CuO}_4$  is a function of temperature and is the highest ( $x = 0.22$ ) at lower annealing temperatures ( $1050^\circ\text{C}$ ). The oxidation state of Cu in the Ce-doped samples was determined by the iodometry method as described elsewhere.<sup>15</sup> The formal valence of Cu is  $2 \pm 0.03$  in  $\text{Nd}_2\text{CuO}_4$  and decreases with increasing Ce content to reach a value of  $1.81 \pm 0.03$  at  $x = 0.2$ . Superconductivity is achieved in this system by annealing the compounds under nitrogen at  $900^\circ\text{C}$  for 14 h and the maximum  $T_c$  (25 K) is obtained for  $x = 0.15$ .  $T_c$  is found to be very dependent upon composition as observed previously.<sup>9,10</sup> Figure 2 shows experimental data for one of our best ceramic samples. The Meissner fraction (not corrected for demagnetization) does not exceed 25% [Fig. 2(a)] and the resistivity temperature dependence is semiconducting-like above  $T_c$  [Fig. 2(b)], both suggesting the presence of inhomogeneities or secondary phases that are not detected by x-ray diffraction.

To obtain more reliable measurements on this system we proceed to grow superconducting Ce-doped  $\text{Nd}_2\text{CuO}_4$  single crystals. To achieve an appropriate crystal growth there are two steps involved: (1) to determine the balance

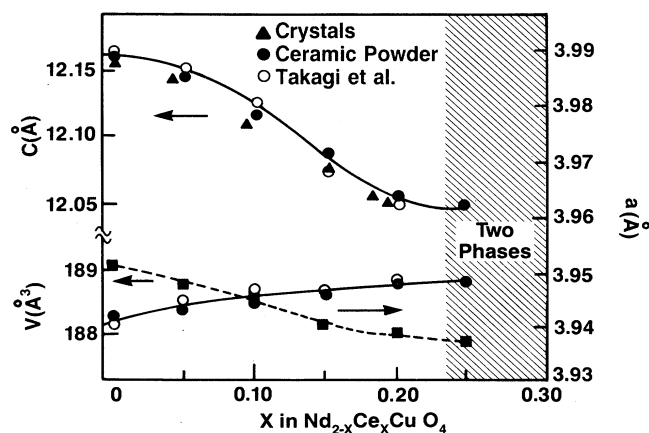


FIG. 1. Variation of the tetragonal crystallographic cell parameters ( $a$  and  $c$ ) and the unit-cell volume ( $V$ ) as a function of  $x$  for the  $\text{Nd}_{2-x}\text{Ce}_x\text{CuO}_4$  system. Solid circles and solid triangles refer to data obtained from ceramic powders and single crystals, respectively. For comparison we also plot (open circles) the powder results of Takagi *et al.*<sup>10</sup>

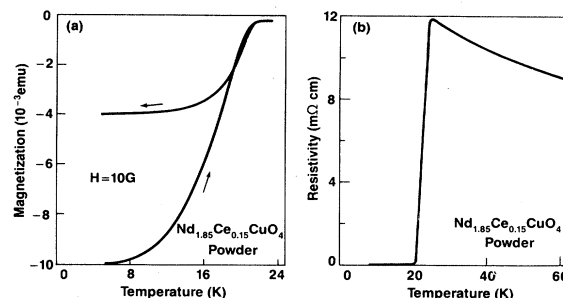


FIG. 2. The Meissner and shielding curves (applied field of 10 G) are shown (a) for a polycrystalline ceramic of composition  $\text{Nd}_{1.85}\text{Ce}_{0.15}\text{CuO}_4$  together with the resistivity measurement (b) for the same sample.

between temperature and ratio of the starting materials so as to obtain the required cerium content (0.15), and (2) to determine the annealing time and temperature to remove the right amount of oxygen (sample reduction) to induce superconductivity.  $\text{Nd}_2\text{CuO}_4$  is chemically similar to  $\text{La}_2\text{CuO}_4$ ; thus, based on previous work<sup>16</sup> done on the growth of Sr-doped  $\text{La}_2\text{CuO}_4$ , we used  $\text{CuO}$  as a flux to grow our Ce-doped  $\text{Nd}_2\text{CuO}_4$  crystals. A number of compositions were reacted at different temperatures so as to survey the range of composition and temperature at which partial melting occurs. Based on the results of this composition-temperature survey we focused on two flux divided by desired composition ratios and two reaction temperatures.

Single crystals of  $\text{Nd}_{2-x}\text{Ce}_x\text{CuO}_4$  were prepared in a platinum crucible using a 20 g charge composed of stoichiometric amounts of  $\text{Nd}_2\text{O}_3$   $[(2-y)/2]$  and  $\text{CeO}_2$  ( $y$ ) and three times the stoichiometric amount of  $\text{CuO}$ . The charge was heated in air at  $180^\circ\text{C}/\text{h}$  to  $1500^\circ\text{C}$ , maintained at this temperature for one hour, and then cooled at  $6^\circ\text{C}/\text{h}$  to  $1100^\circ\text{C}$ , whereupon the sample was removed from the furnace. This treatment partially melts the charge and results in small shiny crystals of the correct phase that are imbedded at the free surface and cannot be separated from the flux. Also, there are cavities at the melt surface which contain nearly free well-defined small crystals. Crystals were collected from charges that contained up to  $y = 0.4$  Ce. The microstructure and Ce composition of the resulting crystals were analyzed using scanning electron microscopy (SEM) and energy dispersive x-ray analysis (EDX). The EDX technique ( $1\mu\text{m}$  spot size) is very sensitive to composition inhomogeneities, but can only give absolute cation concentrations with an accuracy of 3% and requires the use of standards. Here  $\text{Nd}_{2-x}\text{Ce}_x\text{CuO}_4$  ceramic samples were used as standards. SEM on the resulting crystals shows that several of them contain  $\text{CuO}$  inclusions. Using EDX normal to a platelet face we observe that Ce is uniformly distributed (variations in the  $c$ -axis direction would be averaged) throughout the crystal, but the concentration of Ce is low with  $x$  never exceeding  $0.12 \pm 0.1$  even when  $y = 0.4$  Ce in the charge. The  $x$  value is too low to induce superconductivity. To extend the solubility range ( $x$ ) of

Ce we lowered the crystal growing temperature, which required lowering the partial melting temperature of the charge. This was done through the use of additional CuO. Lowering the growing temperature could also help to decrease the number of CuO inclusions because the growth rate is slower.

Single crystals having a Ce content greater than 0.12 were prepared by heating, in an alumina crucible (1.25 cm in diameter and 5-cm high), a 10-g charge composed of stoichiometric amounts of neodymium and cerium oxides as before and with the CuO being five times in excess. The charge was heated in air at a rate of 160°C/h to 1300°C, maintained at this temperature for 1.5 h, then cooled at 6°C/h to 1000°C, whereupon the sample was removed from the furnace. At 1300°C the CuO flux will rapidly climb (due to capillarity) and spill over the crucible lip. This is alleviated by placing the charge-carrying crucible in a wider and shorter alumina crucible, thereby creating a temperature gradient on the inside crucible (hotter at the bottom) in such a way that the CuO remains in the top part of the charge crucible and can still act as a flux. The residual charge at the bottom of the crucible is partially melted and contains, as before, crystals on the surface of cavities [Fig. 3(a)]. The resulting crystals are still frequently contaminated by inclusions of CuO or by the presence of the CuO at the grain boundaries [Fig. 3(b)]. However, from each charge a few crystals free of CuO inclusions [Fig. 3(c)] can be isolated. Using this procedure, crystals as large as  $2 \times 2 \times 0.05$  mm<sup>3</sup> were obtained [Fig. 3(d)]. Thicker crystals (up to 0.1 mm) can be grown by longer annealing (4 h) at 1330°C. With our growth technique, crystals having values of  $x$  ranging from 0 to  $0.18 \pm 0.01$  were obtained. The  $c$  axis is perpendicular to the plate face (parallel to the short dimension) as demonstrated by an x-ray diffraction pattern of a crystal placed face to face on a quartz slide (maintaining Bragg-Brentano geometry) exhibiting only the 001 reflections [Fig. 4(b)]. The  $c$  lattice parameter, determined by the position of the 001 Bragg peaks, for crystals having various Ce contents is shown in Fig. 4. The results are similar to those obtained on ceramic samples. At the growing temperature of 1300°C the maximum solubility (independent of any excess of Ce in the charge) was found to be  $x = 0.18 \pm 0.01$ . This corresponds to the upper Ce composition limit for which superconductivity can exist in this system. The crystals of composition  $x = 0.14$  and  $x = 0.16$  reported in the following were obtained from melts having nominal Ce compositions of  $y = 0.29$  and  $y = 0.33$ , respectively. Having achieved the required Ce content in the crystals, they were then annealed under nitrogen to induce superconductivity.

Thermogravimetric analysis (TGA) measurements are made to determine how the  $\text{Nd}_{2-x}\text{Ce}_x\text{CuO}_4$  compound is affected by the nitrogen ambient in order to optimize the reducing conditions (i.e., determine the annealing temperature) for producing superconductivity. Figure 5 shows the TGA traces for crystals of composition  $x = 0.16$  heated in nitrogen (curve *a*), subsequently cooled in nitrogen and then reheated under oxygen up to 900°C using a heating rate of 5°C/min (curve *b*). Most of the weight

loss or gain takes place at temperatures above 700°C. Curve *a* shows that the loss of oxygen mainly occurs within the range of temperature 720–900°C when the sample is heated (in nitrogen), but we note (not shown in Fig. 5) that a plateau is reached only for temperatures greater than 1000°C. Curve *b* shows that the sample re-

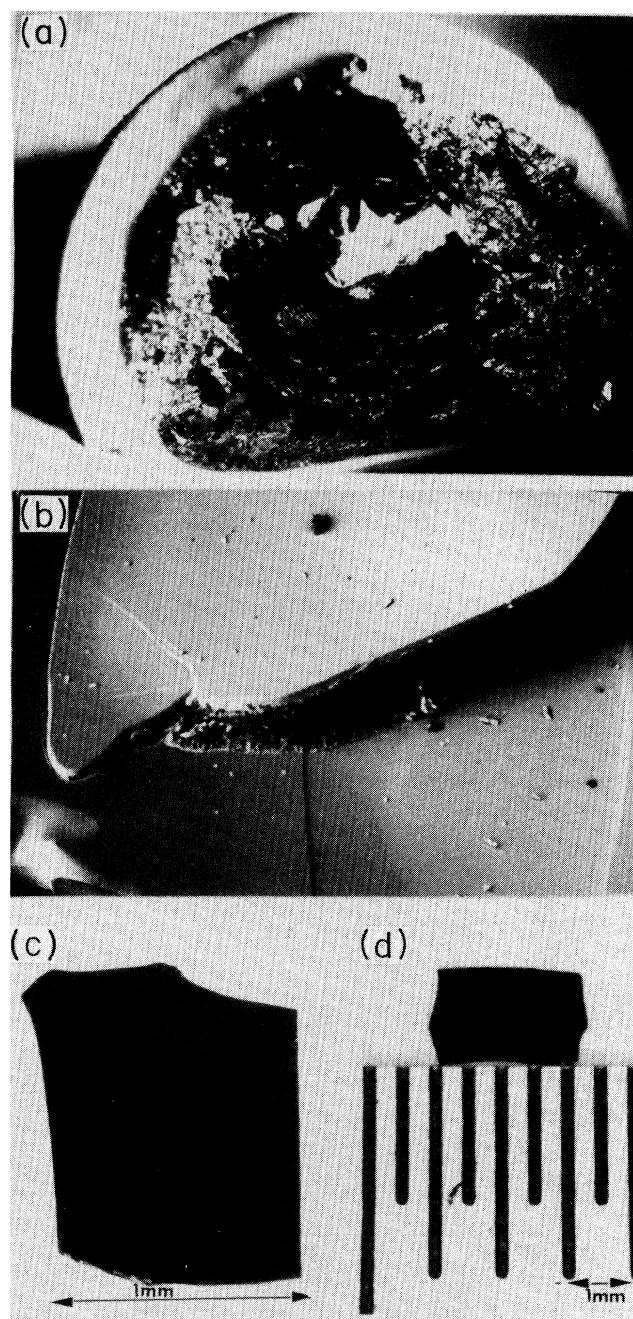


FIG. 3. Growth of  $\text{Nd}_{2-x}\text{Ce}_x\text{CuO}_4$  crystals. We show (a) crystals within the CuO flux, (b) the presence of CuO as an inclusion at the cleaved surface, (c) low magnification picture of the crystal "mirrorlike" surface, and (d) the shape and dimensions of one of the best crystals grown thus far.

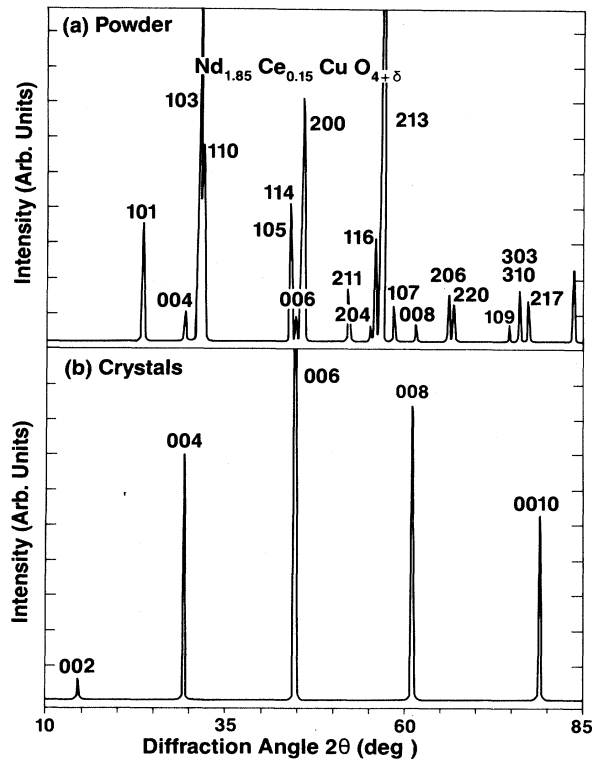


FIG. 4. X-ray diffraction patterns of a ceramic of composition  $\text{Nd}_{1.85}\text{Ce}_{0.15}\text{CuO}_4$  (a) and of a *c*-oriented crystal (b) of the same composition are shown. The Miller indices are noted above each peak.

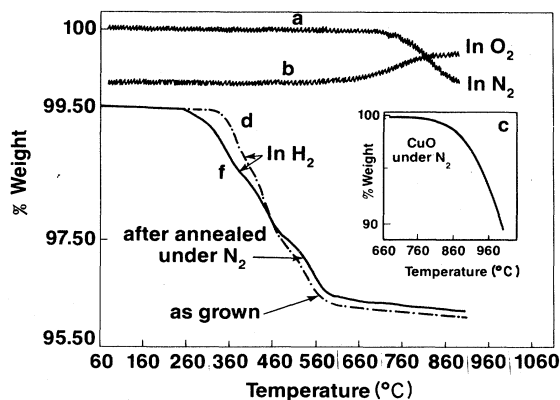


FIG. 5. Thermal analysis of the  $\text{Nd}_{2-x}\text{Ce}_x\text{CuO}_4$  ( $x=0.16$ ) crystals. Curve *a* shows the weight lost by the crystals when heated in nitrogen and curve *b* shows the weight gained when heated in oxygen. The weight loss due to the reduction under a  $\text{H}_2/\text{Ar}$  mixture at 900 °C for the crystals as grown and after their treatment under nitrogen are shown as *c* and *d*, respectively. The inset shows, for reasons described in the text, the reduction of CuO under nitrogen.

covers most of its oxygen content when heated (in oxygen) over the same temperature range. However, from measurements on several batches of crystals or powders we observe that the weight loss is always reproducibly greater than the weight gain. This suggests that there is a slight volatilization of one component. The range of oxygen nonstoichiometry in this material is 0.04 atoms per unit formula, as determined by the weight gain in oxygen observed in Fig. 5, curve *b*. This value could be slightly overestimated because of the CuO inclusions in some of the crystals. Note that the temperature range over which the reduction of CuO by nitrogen occurs (Fig. 5 inset) overlaps with the temperature range over which the  $\text{Nd}_{2-x}\text{Ce}_x\text{CuO}_4$  is reduced. The total oxygen content per unit formula was determined from the weight loss of the crystals when heated in a reducing  $\text{H}_2/\text{Ar}$  ambient up to 900 °C at a rate of 5 °C/min. We determined an oxygen content of 4.01 per unit formula ( $\text{Nd}_{1.84}\text{Ce}_{0.16}\text{CuO}_4$ ) for the as-grown crystals (curve *d*) and 3.97 for the crystals after being annealed under nitrogen with, therefore, a difference of 0.04. Identical results were obtained by performing the measurements on a 0.15 Ce-doped powder sample. This range of nonstoichiometry in oxygen can be extended by using other synthesis conditions. For instance, we found that for an  $x=0.15$  Ce-doped sample the oxygen content can be increased to 4.03 by heating the as-grown material under 80 bars of oxygen at  $T=800^\circ\text{C}$ , or lowered to 3.96 by annealing the same material under nitrogen at 1000 °C for 15 h. Under these extreme conditions decomposition reactions leading to secondary phases could be possible, but no evidence for decomposition was detected by x-ray diffraction on samples heated to 800 °C under oxygen pressure, or to 1000 °C under nitrogen. Only slight changes of the *c* axis and unit-cell volume, *V*, were observed between the oxygen and nitrogen treated samples; e.g., for an  $x=0.15$  nitrogen annealed sample *c* and *V* increase from  $c=12.078 \text{ \AA}$  and  $V=187.85 \text{ \AA}^3$  to  $c=12.083 \text{ \AA}$  and  $V=188.03 \text{ \AA}^3$  as the sample is treated under oxygen pressure.

Superconductivity is induced in these materials by removal of oxygen, thus the TGA results suggest that superconductivity should be induced only for those annealing temperatures greater than 750 °C (beginning of the oxygen loss). Crystals from the same batch ( $x=0.16$ ) were annealed at temperatures of either 700 or 860 °C for 60 h. As expected after such a treatment, the crystals heated at 700 °C were not superconductors, whereas those annealed at 860 °C were. Reannealing the nonsuperconducting crystals (previously annealed at 700 °C) at 860 °C for 14 h induces superconductivity. We also note that the annealing of superconducting samples at higher temperatures (1000 °C) under nitrogen destroys superconductivity. This observation, together with the fact that the oxygen loss is not complete by 900 °C in these materials, indicates that there is a critical oxygen composition for which the sample becomes fully superconducting, but this critical oxygen content does not correspond to that for a fully reduced sample. This points out a major difficulty to be faced in removing oxygen homogeneously from the crystals. Although oxygen homogeneity is a problem during the crystal growth of the 123 material,

the superconducting phase corresponds to the fully oxidized phase so that longer annealing times will always be beneficial.<sup>17</sup> In contrast, with the Ce-doped neodymium samples there is a subtle balance between annealing temperatures and times. Unless otherwise noted our reducing thermal treatment consists of heating (for all Ce contents) the crystals in nitrogen at 900 °C for 24 h. According to Fig. 5, this corresponds to an oxygen loss of 0.04.

Superconductivity was determined by measuring the Meissner expelled flux and the shielding effect using a superconducting quantum interference device (SQUID). A series of crystals with compositions ranging from 0 to 0.18 were investigated. Only those with  $x$  in the composition range (0.14–0.17) were superconductors in agreement with the results established by Takagi *et al.*<sup>10</sup> on ceramic samples. Figure 6 shows the Meissner and shielding effects for a single crystal (1.3 mg) of composition  $x = 0.14$  (curve *a*) and for 3 crystals (total weight 2.1 mg) of composition  $x = 0.16$  (curve *b*). The  $x = 0.14$  sample was cooled in zero field, warmed in a field of 5 G (Shielding), and then cooled in a 5-G field (Meissner), whereas an applied field of 10 G was used for the  $x = 0.16$  sample. In each case, the applied field is parallel to the  $c$ -crystallographic direction. For each  $\text{Nd}_{2-x}\text{Ce}_x\text{CuO}_4$  crystal, the Meissner and shielding curves indicate equivalent superconducting temperature onsets of about 16 K and 21 K for  $x = 0.16$  and  $x = 0.14$ , respectively. However, the superconducting transition is broad and extends to 5 K without reaching a plateau. From the amplitude of the diamagnetization signal and assuming that the crystals have a density of 7.6 g/cm<sup>3</sup>, we deduce (without correcting for the demagnetization factor) a Meissner fraction at  $T = 5$  K of 40% for the  $x = 0.16$  sample and 60% for the  $x = 0.14$  sample. These large Meissner values demonstrate bulk superconductivity in these materials. However, the width of the superconducting transition suggests inhomogeneities, as discussed in the following.

Resistivity from room temperature to 4.2 K on the same crystals as those used for the magnetic measurements is shown in Fig. 7. Four-probe measurements, ei-

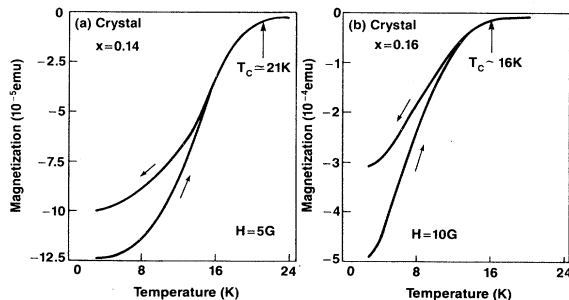


FIG. 6. Magnetization vs temperature for  $\text{Nd}_{2-x}\text{Ce}_x\text{CuO}_4$  crystals of composition  $x = 0.14$  (curve *a*) and  $x = 0.016$  (curve *b*). The upper curves are for cooling in a constant field (Meissner) whereas the lower curves are for heating in the same constant field (shielding). Fields of 5 G and 10 G were used for the  $x = 0.14$  and  $x = 0.16$  crystals, respectively.

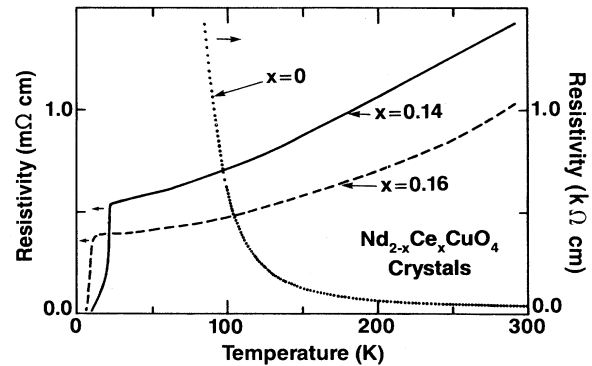


FIG. 7. Resistivity vs temperature from 5 to 300 K measured on the same  $\text{Nd}_{2-x}\text{Ce}_x\text{CuO}_4$  crystals ( $x = 0.14$  and 0.16) as those used for the magnetic measurements. Also shown are data for an undoped  $\text{Nd}_2\text{CuO}_4$  crystal. Note the  $10^6$  scale change between the metalliclike superconductor and the semiconductor data.

ther in-line or in a van der Pauw geometry in the  $a$ - $b$  plane are done in a liquid helium, exchange gas cryostat with a Si-diode thermometer (standard 0.2 K calibration) buried in the Cu-block sample holder. Below 40 K, a Ge-resistance thermometer (0.05-K calibration) was also used. Varying the alternating current from 3 mA down to 1  $\mu\text{A}$  on these crystals did not (to the accuracy of our measurements) affect the absolute resistivity, even below the onset of the superconducting transition. Because of the crystal sizes (0.25 to 1.5 mm on a side and 20–40  $\mu\text{m}$  thick) and irregular shapes, the absolute value of the resistivity is calculated to no better than 20%. Low resistance contacts, reproducibly in the 10–70  $\Omega$  range, are made by soldering four In(Ag) spots in the crystal. Leads of 0.5-mm thick Al foil cut into thin strips are then silver epoxied to these contacts and cured for  $\frac{1}{2}$  h at 125 °C. Note that the temperature-dependent resistivity is metalliclike and, like the  $p$ -type high-temperature superconducting cuprates, is linear above 150 K. A striking difference from the 214, 123, and 2212 systems is that the resistivity here approached an impurity-dominated regime at low temperatures. For our crystals with the highest resistance ratios  $\{[R(290 \text{ K})/R(25 \text{ K})]$ , typically 2.6 to 2.8 $\}$ , the in-plane resistivity is 450  $\mu\Omega \text{ cm}$  at room temperature, as determined by the van der Pauw method. The superconducting onsets measured resistively for the single crystals of composition  $x = 0.14$  and 0.16 are 22 K and 15 K, respectively. These results are consistent with our magnetization measurements with the exception that with such a large Meissner fraction, zero resistance is expected to be achieved. Here, the superconducting transition is broadened such that zero resistance (ac voltage drop less than 100 nV over a  $\sim 0.5$  mm length) is never observed, even down to 2.5 K. Zero resistance has not been observed in any of the more than 40 crystals (grown from several different batches) measured, indicating that this may be an intrinsic property of crystals prepared in the manner described. We address this point in the discussion section but we note here the

similarity to the complex Bi-based system in which samples with more than 50% of the 110 K phase (2223) did not show zero resistance until 85 K.<sup>18,19</sup> The Hall coefficient measured on these crystals is negative with

values at 80 and 120 K close to those reported for ceramic samples.<sup>10</sup> A detailed report will be published elsewhere. Also in Fig. 7 is plotted the temperature-dependent resistivity for an undoped  $\text{Nd}_2\text{CuO}_4$  crystal.

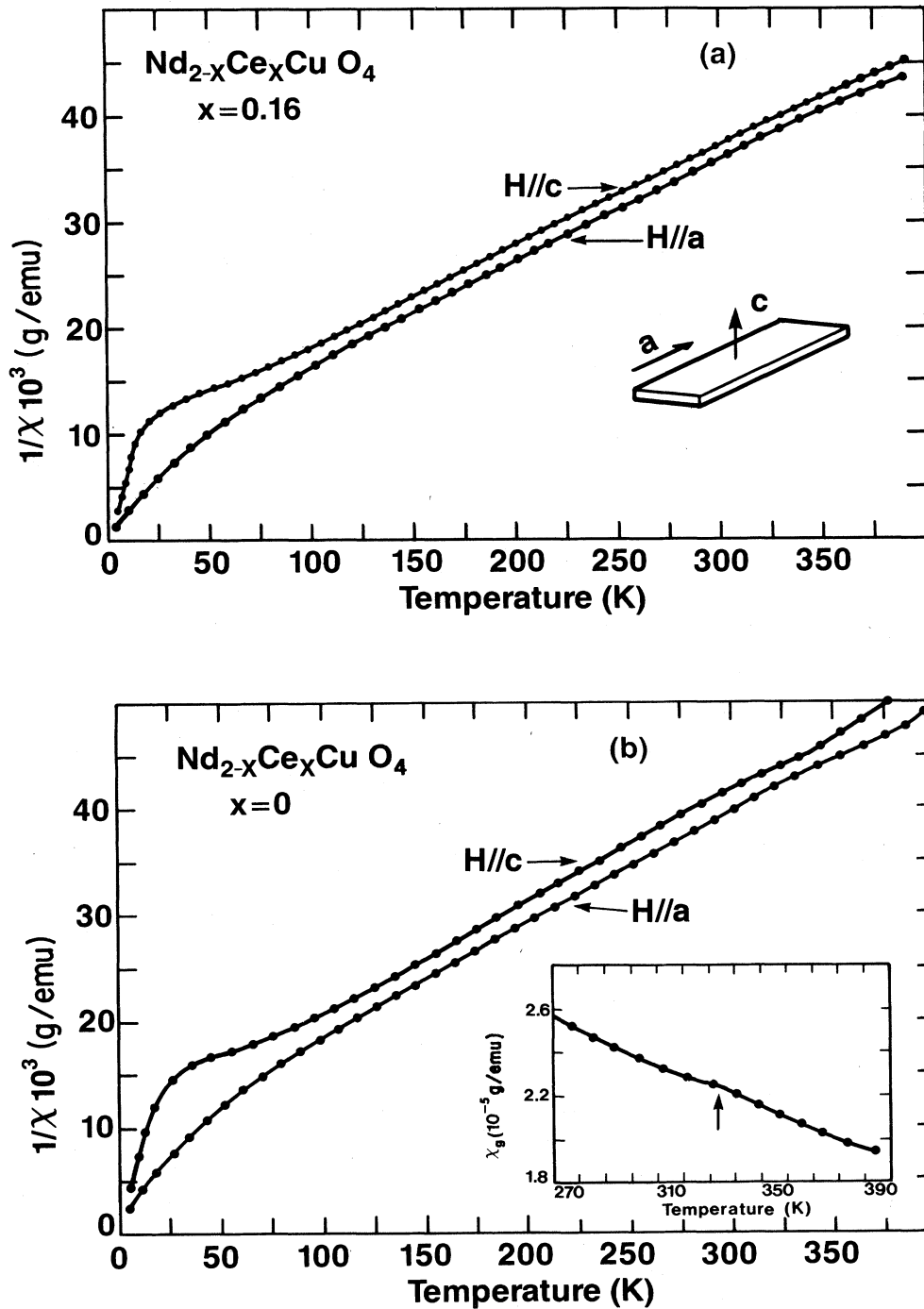


FIG. 8. The temperature dependence of the inverse susceptibility is shown for a doped  $\text{Nd}_{2-x}\text{Ce}_x\text{CuO}_4$  single crystal of composition  $x=0.16$  ( $T_c = 15 \text{ K}$ ) (a) and an undoped  $\text{Nd}_2\text{CuO}_4$  single crystal (b), with the applied magnetic field (10 kG) parallel and perpendicular to the crystallographic  $c$  axis. For  $\text{Nd}_2\text{CuO}_4$  the susceptibility temperature dependence is also plotted for  $H$  parallel to  $c$  (inset) for the region of temperatures at which an anomaly in the  $1/\chi$  vs  $T$  is observed.

Note that the room-temperature resistivity is  $\sim 2 \times 10^5$  times greater than that of the superconductor and the temperature dependence is like that of an insulating semiconductor. No resistive anomalies were observed up to 340 K.

Magnetic measurements were performed from 4.2 to 390 K in an applied field of 10 kG on the  $x = 0.15$  crystal prior to its treatment in nitrogen (nonsuperconducting) and after (superconducting) using a SQUID magnetometer. The results being identical at this applied field, we show only the data obtained for the superconducting crystal. In analyzing the data we assume (1) that in the Ce-doped  $\text{Nd}_2\text{CuO}_4$  the  $\text{Cu}^{2+}$  ions are not magnetic, and (2) that the Ce ions are tetravalent, so they also are diamagnetic. In other words, we assume that only the Nd atoms are responsible for the paramagnetic susceptibility in the Ce-doped materials. Measurements were made with the applied field (10 kG) both parallel and perpendicular to the crystallographic  $c$  axis. The susceptibility temperature dependence of the  $x = 0.16$  [Fig. 8(a)] shows anisotropy. When the field is parallel to the  $c$  axis the inverse susceptibility behaves in a different manner in different temperature regions. For instance, we fit the susceptibility to a Curie-Weiss law of the general form  $\chi_g = C_g / (T + \Theta_p) + \chi_0$  over the range of temperature 100–300 K with a root-mean-square deviation ( $\sigma$ ) of 0.0017. A  $\Theta_p$  (paramagnetic Curie temperature) of 70 K and a  $C_g$  (Curie constant) of 0.008 265 were obtained from the preceding fit, which leads to a  $\mu_{\text{eff}}$  of  $3.85 \mu_B$  per Nd atom (assuming that only  $\text{Nd}^{3+}$  ions are responsible for magnetism in this system). For temperatures lower than 100 K,  $1/\chi$  flattens out, and then from 20 to 2 K, changes linearly with  $T$ . Over this range of temperatures (20–2 K) a Curie-Weiss law fit ( $\sigma = 0.003$ ) yields  $\Theta_p = -1\text{K}$ ,  $C_g = 0.001\ 06$ , and  $\mu_{\text{eff}} = 1.4 \mu_B$  per Nd atom. Another interesting feature of Fig. 8 is the slight upturn of  $1/\chi$  (over the temperature range 30–50 K) above the extrapolation of the high-temperature part. This feature is absent when the applied field is perpendicular to the  $c$  axis. In this later case the inverse susceptibility temperature dependence shows a crystal-field-induced curvature which extends up to 120 K. From 120 to 320 K the behavior follows a Curie-Weiss law with parameters similar to those obtained from the high-temperature susceptibility when the applied field was parallel to  $c$ .

The magnetic behavior for an undoped  $\text{Nd}_2\text{CuO}_4$  single crystal (1.8 mg) is shown in Fig. 8(b). The inverse susceptibility depends strongly upon the orientation of the applied field. When the field is parallel to  $c$  the data were analyzed in the same way as before and two ranges of temperature, 2–25 K and 100–300 K, were found to fit a Curie-Weiss law with  $\Theta_p$  of 1 K and 78 K, respectively. When  $1/\chi$  is extrapolated from high temperatures, a deviation at low temperatures (in the form of a slight upturn) is still present. This is in contrast to early work on ceramic samples.<sup>20</sup> The most interesting feature of the magnetic data [Fig. 8(b)] for the undoped material is the broad anomaly near 340 K (more pronounced when  $H$  is parallel to the crystallographic  $c$  axis) in the inverse susceptibility temperature dependence most likely associated with an antiferromagnetic ordering of the  $\text{Cu}^{2+}$  ions.

Such a feature was not observed for the Ce-doped sample. This finding supports the muon spin resonance work<sup>21</sup> which indicates that a magnetic ordering is taking place in the  $\text{Nd}_2\text{CuO}_4$  at temperatures close to room temperature. This is also in agreement with previous magnetic studies by Saez Puche *et al.*<sup>20,22</sup> on undoped  $\text{Nd}_2\text{CuO}_4$  ceramic samples which lead to the conclusion that this compound is a planar copper antiferromagnet. However, neutron scattering experiments remain to be done to confirm unambiguously the magnetic ordering associated with the Cu ions. Saez Puche *et al.* also found that for a  $\text{Nd}_2\text{CuO}_4$  powder sample the susceptibility temperature dependence changes from a Curie-Weiss law at high temperatures ( $T > 30$  K) to a near-Curie law at low temperatures ( $T < 30$  K), similar to that reported here for the Ce-doped or undoped crystals. It is interesting that the shape of  $1/\chi$  versus  $T$  obtained on single crystals when  $H$  is perpendicular to  $c$  is identical to that calculated for an isolated  $\text{Nd}^{3+}$  ion under the influence of a cubic crystal field, assuming that only the levels resulting from the splitting of the lowest multiplet level,  $^4I_{9/2}$ , are thermally populated and that the exchange interactions between  $\text{Nd}^{3+}$  ions are unimportant (see Fig. 3 of Ref. 20). Finally the anisotropy in the inverse susceptibility temperature dependence for both doped and undoped crystals could arise from an anisotropy in the magnetic field splitting (i.e., a separation between the energy levels which results from the applied magnetic field and is a function of its direction) as in  $\text{Eu}_2\text{CuO}_4$  (Ref. 23).

## DISCUSSION

We described the growth of  $\text{Nd}_{2-x}\text{Ce}_x\text{CuO}_4$  single crystals using CuO in large excess as a flux and have shown that bulk superconductivity exists in this system for  $0.14 \leq x \leq 0.17$ . The crystal structure of the undoped parent compound  $\text{Nd}_2\text{CuO}_4$  (called the  $T'$  phase) is closely related to that of  $\text{La}_2\text{CuO}_4$  with the main difference being that in the  $T'$  phase the Cu is in a square planar environment<sup>24</sup> instead of the octahedral coordination as in  $\text{La}_2\text{CuO}_4$  (i.e., there is no apical oxygen). This structural difference may be the origin of the different physical and chemical behavior observed for the Sr-doped La-Cu-O and the Ce-doped Nd-Cu-O systems.

The Nd-Cu-O system has a range of oxygen non-stoichiometry similar to that found for  $\text{La}_2\text{CuO}_4$  (0.04 per unit formula). However, the uptake or removal of oxygen is more difficult for the Nd-based material than for the La phase<sup>8,25</sup> in that the gain or loss of oxygen occurs at higher temperatures for the Nd-based materials (750°C) than for the La phase (500°C). Similarly we were able to introduce oxygen, and thereby induce superconductivity, in the La phase by plasma oxidation near room temperature.<sup>26</sup> In contrast, reintercalating oxygen (and thereby destroying superconductivity) in a nitrogen annealed superconducting Nd-based sample was not possible even after plasma oxidation times as long as 156 h. This indicates that diffusion is the rate limiting factor for the insertion of oxygen into these materials and that the diffusion is faster in the La than the Nd phase. In the La system it is possible, through the use of high pressures

(100 bars) or plasma oxidation, to achieve an oxygen content of 4.08 (Ref. 27), whereas with the Nd phase (using the same procedures) we were unable to reach oxygen contents greater than  $4.03 \pm 0.01$ . Another interesting observation is that reducing this material under nitrogen (i.e., removing oxygen) at 900°C induces superconductivity, whereas further annealing at 1000°C destroys it with apparently no evidence for decomposition as determined by x-ray diffraction. There are two types of oxygen sites (in the  $\text{CuO}_2$  planes and between the Nd layers) in this structure. It is possible that at 900°C the oxygen is removed primarily from the Nd layers, and at higher temperatures oxygen from the  $\text{CuO}_2$  planes may also be removed. Introducing crystallographic disorder, especially in the  $\text{CuO}_2$  planes, would suppress superconductivity, as we have stated previously for the other high- $T_c$  systems.<sup>28</sup>

We now discuss our unexpected observation that it is difficult to obtain zero resistance with a four-point probe measurement down to 2.5 K on crystals which have a well-defined crystallographic habit, "mirrorlike" surfaces, and, importantly, a large Meissner fraction. Often crystals of  $\text{La}_{2-x}\text{Sr}_x\text{CuO}_4$  and  $\text{Bi}_4\text{Sr}_4\text{Ca}_2\text{Cu}_4\text{O}_y$  grown from a CuO flux have a  $T_c$  onset that is lower and a  $\Delta T_c$  which is broader than that observed in bulk phases (e.g., ceramic compacts) of the same material.<sup>29,30</sup> This is generally attributed, without direct experimental verification, to a variation in composition such as a dopant cation or oxygen. Certainly such an explanation could also apply to our doped Nd-based crystals and the effects would be more marked because of the lower  $T_c$  in this system. However, we offer a different, additional explanation which involves a process-induced complex microstructure: The presence of internal defects may entrain CuO during the nucleation and growth in the CuO flux and/or from the condensation of the vapor onto all free surfaces as the crucible is cooled. During the annealing of the crystals under nitrogen the CuO is reduced (as is also the  $\text{Nd}_{2-x}\text{Ce}_x\text{CuO}_4$ ) but, in contrast to the Nd phase, the reduction of the CuO is accompanied by a large change in volume which creates internal strains and microcavities. This is consistent with our observation that the crystals become more fragile after being treated under nitrogen. Crystals that have been annealed at higher temperatures (950°C) are most brittle, and when fracture occurs a reddish hue is observed between lamella parallel to the basal plane indicating the presence of free  $\text{Cu}_2\text{O}$  or elemental Cu. Such a microstructure may account for the large volume Meissner fraction and nonzero resistance down to 4.2 K. We also note that the brittle crystals fracture in a micaceous way. If in fact two-dimensional (2D) percolation is required for conduction, the volume fraction (Meissner fraction) of superconducting material required (0.47) for a continuous path is higher than required in three dimensions.

This new system, which has demonstrated that the hole

carriers are not unique for the occurrence of high-temperature superconductivity in the cuprates, can also be used to examine the role and importance of magnetic interactions. In  $\text{La}_2\text{CuO}_4$ , an antiferromagnetic transition with a ferromagnetic component (leading to a sharp cusp in the susceptibility temperature dependence) associated with a spin canting out of the plane was observed at 250 K (Refs. 30 and 31). It has been shown that the two main requirements for this spin canting are an interlayer coupling and an antisymmetric exchange (orthorhombic unit cell).  $\text{Nd}_2\text{CuO}_4$  is tetragonal and there is no apical oxygen (Cu is square planar); thus one would expect different magnetic interactions than those in  $\text{La}_2\text{CuO}_4$  with, in particular, a more pronounced 2D character of the  $\text{CuO}_2$  sheets. Also, no sharp cusp in the susceptibility data due to spin canting (as observed in  $\text{La}_2\text{CuO}_4$ ) should be observed for  $\text{Nd}_2\text{CuO}_4$  since there is no antisymmetric exchange. This is consistent with our susceptibility results which have shown no sharp features, but rather a broad anomaly at  $\sim 340$  K.

In  $\text{La}_2\text{CuO}_4$  the substitution of La by Sr suppresses the magnetic ordering and induces superconductivity. We show here for the Nd-Ce-Cu-O system that, as the neodymium is replaced by cerium, the compound becomes more metalliclike and the anomaly in the susceptibility at 340 K (associated with an ordering of the Cu ions) present in  $\text{Nd}_2\text{CuO}_4$  at 340 K vanishes. Thus we conclude that, with respect to their magnetic behavior,  $n$ -type or  $p$ -type materials are strikingly similar since in both systems the parent compounds are antiferromagnetic insulators and either  $p$ - or  $n$ -type substitution destroys magnetic interactions and induces superconductivity (a relevant result which may distinguish theoretical models that emphasize the importance of magnetic interactions for the pairing mechanism). Magnetic ordering of Cu is present in both undoped La and Nd compounds. Thus, as in  $\text{La}_2\text{CuO}_4$ , neutron experiments on single crystals need be done to determine the  $\text{Nd}_2\text{CuO}_4$  magnetic behavior. Finally, we note that in  $\text{La}_{2-x}\text{Sr}_x\text{CuO}_4$  a maximum  $T_c$  is obtained at strontium contents,  $x$ , in the range 0.15–0.21, i.e., 0.15–0.21 holes per unit formula. In the  $\text{Nd}_{2-x}\text{Ce}_x\text{CuO}_{4-y}$  system the maximum  $T_c$  occurs in the region  $x \cong 0.15$  and  $y \cong 0.04$  or at an electron doping level of  $\sim 0.23$  per unit formula. Thus we find it interesting that the maximum  $T_c$  occurs in  $n$ -type materials at the same electron concentration as the hole concentration in  $p$ -type materials which produces a maximum in  $T_c$ . Further work should resolve whether this intriguing doping symmetry is a basic property of the material.

#### ACKNOWLEDGMENTS

We wish to thank C. C. Chang, V. Emery, W. L. Feldmann, S. Gregory, M. S. Hedge, P. L. Key, W. R. McKinnon, R. Ramesh, J. M. Rowell, M. Tinkham, and J. H. Wernick for valuable discussions.



- <sup>1</sup>J. G. Bednorz and K. A. Muller, *Z. Phys. B* **64**, 189 (1986).
- <sup>2</sup>M. K. Wu, J. R. Ashburn, C. J. Torng, P. H. Hor, R. L. Meng, L. Gao, Z. J. Huang, Y. Q. Wang, and C. W. Chu, *Phys. Rev. Lett.* **58**, 908 (1987).
- <sup>3</sup>H. Maeda, Y. Tanaka, M. Fukutumi, and T. Asano, *Jpn. J. Appl. Phys.* **27**, L209 (1988).
- <sup>4</sup>Z. Z. Cheng and A. M. Herman, *Nature (London)* **332**, 55 (1988); **332**, 138 (1988).
- <sup>5</sup>S. S. Parkin, V. Y. Lee, E. M. Engler, A. I. Nazzari, T. C. Huang, G. Gorman, R. Savoy, and R. Beyers, *Phys. Rev. Lett.* **60**, 2539 (1988).
- <sup>6</sup>K. Kishio, K. Kitazawa, S. Kanbe, I. Yasuda, N. Sugil, H. Takagi, S. Uchida, K. Fueki, and S. Tanaka, *Chem. Lett.* **489** (1987).
- <sup>7</sup>R. J. Cava, R. D. van Dover, B. Batlogg, and E. A. Rietman, *Phys. Rev. Lett.* **58**, 408 (1987).
- <sup>8</sup>J. M. Tarascon, L. H. Greene, W. R. McKinnon, G. W. Hull, and T. H. Geballe, *Science* **235**, 1373 (1987).
- <sup>9</sup>T. Tokura, H. Takagi, and S. Uchida, *Nature* **337**, 345 (1989).
- <sup>10</sup>H. Takagi, S. Uchida, and Y. Tokura, *Phys. Rev. Lett.* **62**, 1197 (1989).
- <sup>11</sup>J. M. Tranquada, S. M. Heald, A. R. Moodenbaugh, G. Liang, and M. Croft, *Nature* **337**, 720 (1989).
- <sup>12</sup>A. James, D. W. Murphy, and S. Zahurak, *Nature* (to be published).
- <sup>13</sup>J. T. Markert and B. Maple, *Solid State Commun.* (to be published).
- <sup>14</sup>J. T. Markert, E. A. Early, T. Bjornholm, S. Ghamaty, B. W. Lee, J. J. Neumeier, R. D. Price, C. L. Seaman, and M. B. Maple, *Physica* (to be published).
- <sup>15</sup>A. Manthiran, J. S. Swinnea, Z. T. Sui, H. Steinfink, and J. B. Goodenough, *J. Am. Chem. Soc.* **109**, 6667 (1987).
- <sup>16</sup>Y. Hidaka, Y. Enomoto, M. Suzuki, M. Oda, and T. Murakami, *J. Cryst. Growth* **85**, 581 (1987).
- <sup>17</sup>D. L. Kaiser, F. Holtzberg, M. F. Chisholm, and T. K. Worthington, *J. Cryst. Growth* **85**, 593 (1987).
- <sup>18</sup>J. M. Tarascon, Y. LePage, P. Barboux, B. G. Bagley, L. H. Greene, W. R. McKinnon, G. W. Hull, M. Giroud, and D. M. Hwang, *Phys. Rev. B* **37**, 9382 (1988).
- <sup>19</sup>J. M. Tarascon, Y. LePage, L. H. Greene, B. G. Bagley, P. Barboux, D. M. Hwang, G. W. Hull, W. R. McKinnon, and M. Giroud, *Phys. Rev. B* **38**, 2504 (1988).
- <sup>20</sup>R. Saez Puche, M. Norton, T. R. White, and W. S. Glaunsinger, *J. Solid State Chem.* **50**, 281 (1983).
- <sup>21</sup>G. M. Luke, B. J. Sternlieb, Y. J. Uemura, J. H. Brewer, R. Kadono, R. F. Kiefl, S. R. Kretzmann, T. M. Riseman, J. Gopalakrishnan, A. W. Sleight, M. A. Subramanian, S. Uchida, H. Takagi, and Y. Tokura, *Nature* **338**, 49 (1989).
- <sup>22</sup>R. Saez Puche, M. Norton, and W. S. Glaunsinger, *Mater. Res. Bull.* **17**, 1523 (1982).
- <sup>23</sup>M. Tovar, D. Rao, J. Barnett, S. B. Oseroff, J. D. Thompson, S. W. Cheong, Z. Fisk, D. C. Vier, and S. Schultz, *Phys. Rev. B* **39**, 2661 (1989).
- <sup>24</sup>H. Muller-Buschbaum, *Angew. Chem. Int. Ed. Engl.* **16**, 674 (1977).
- <sup>25</sup>E. M. Vogel, G. W. Hull, and J. M. Tarascon, *Math. Lett.* **6**, 269 (1988).
- <sup>26</sup>B. G. Bagley, L. H. Greene, J. M. Tarascon, and G. W. Hull, *Appl. Phys. Lett.* **51**, 622 (1987).
- <sup>27</sup>J. D. Jorgensen, B. Dabrowski, Shiyou Pei, D. G. Hinks, L. Soderholm, B. Morosin, J. E. Shirber, E. L. Venturini, and D. S. Ginley, *Phys. Rev. B* **38**, 1137 (1988).
- <sup>28</sup>L. H. Greene, J. N. Tarascon, B. G. Bagley, P. Barboux, W. R. McKinnon, and G. W. Hull, *Rev. Solid State Sci.* **1**, 199 (1987).
- <sup>29</sup>P. A. Morris, W. A. Bonner, B. G. Bagley, G. W. Hull, N. G. Stoffel, L. H. Greene, B. Meagher, and M. Giroud, *Appl. Phys. Lett.* **53**, 249 (1988).
- <sup>30</sup>R. J. Birgeneau and G. Shirane, in *Physical Properties of High Temperature Superconductors*, edited by D. M. Ginsberg (World-Scientific, Singapore, 1989).
- <sup>31</sup>T. Thio, T. R. Thurston, N. W. Preyer, P. J. Picone, M. A. Kastner, H. P. Jenssen, D. R. Gabbe, C. Y. Chen, R. J. Birgeneau, and A. Aharony, *Phys. Rev. B* **38**, 905 (1988).

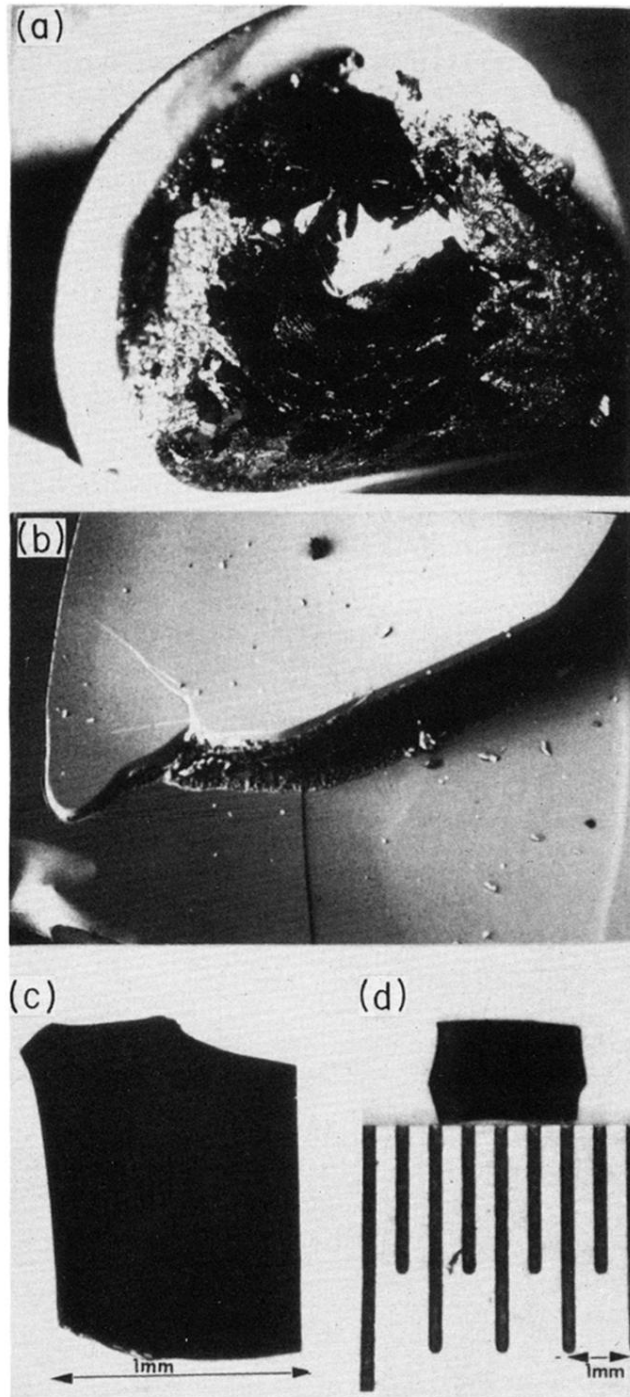


FIG. 3. Growth of  $\text{Nd}_{2-x}\text{Ce}_x\text{CuO}_4$  crystals. We show (a) crystals within the CuO flux, (b) the presence of CuO as an inclusion at the cleaved surface, (c) low magnification picture of the crystal "mirrorlike" surface, and (d) the shape and dimensions of one of the best crystals grown thus far.